RESEARCH ARTICLE

Macromolecular Rapid Communications
www.mrc-journal.de

Polymer-Grafted Nanoparticles (PGNs) with Adjustable Graft-Density and Interparticle Hydrogen Bonding Interaction

*Chenyun Yuan, Florian Käfer, and Christopher K. Ober**

Polymer-grafted nanoparticles (PGNs) receive great attention because they possess the advantages of both the grafted polymer and inorganic cores, and thus demonstrate superior optical, electronic, and mechanical properties. Thus, PGNs with tailorable interparticle interactions are indispensable for the formation of a superlattice with a defined and ordered structure. In this work, the synthesis of PGNs is reported which can form interparticle hydrogen-bonding to enhance the formation of well-defined 2D nanoparticle arrays. Various polymers, including poly(4-vinyl pyridine) (P4VP), poly(dimethyl aminoethyl acrylate) (PDMAEMA), and poly(4-acetoxy styrene) (PAcS), are attached to silica cores by a "grafting from" in a mini emulsion-like synthesis approach. SiO_2-PAcS brushes are deprotected by hydrazinolysis and converted into poly(4-vinyl phenol) (PVP), containing hydroxyl groups as potential hydrogen-bonding donor sites. Understanding and controlling interparticle interactions by varying grafting density in the range of 10^{-2}–10^{-3} chain nm^{-2}, and the formation of interparticle hydrogen bonding relevant for self-assembly of PGNs and potential formation of PGN superlattice structures are the motivations for this study.

1. Introduction

Colloidal monodisperse materials, both polymeric and organic/inorganic composite materials, are of interest for a wide range of applications due to their optical and mechanical properties and their self-assembly in 2D and 3D superlattice structures, for use as optical switches and chemical sensing. [1–4] Zentel et al. describe the synthesis of monodisperse methacrylate colloids (MMA, *tert*-butyl methacrylate, and 2,2,2-trifluoro ethyl methacrylate) with a diameter of several hundred nm for the preparation of polymer opals as photonic crystals.[5–7] In this work, a surfactant-free emulsion polymerization (SFEP) was investigated showing the early formation of seed particles and their continuous swelling until all monomer is consumed. However, the synthesis of polymeric nanoparticles and organic/inorganic nano-colloids require a more controllable synthesis approach to precisely produce a desired morphology, i.e., size and shape. Emulsion-, mini-emulsion, and surface-initiated polymerization in dispersion and emulsion are widely used techniques for the synthesis of those nanoparticles.[8] Thereby, the localization of the polymerization has a significant effect on the particle dispersity, the formation of a homogeneous polymer corona on inorganic core materials, and the formation of unwanted side products such as short polymer chains or ungrafted polymer.

PGNs consist of a core, mostly derived from metals or other inorganic materials such as oxides with polymer chains grafted to the core surface. The high processability of polymers and the tunable corona properties make the single-component composite system attractive to the research community.[9–11]

Among different PGN synthesis strategies, the "grafting from" approach is known to offer good control over the structure of the PGNs, where the bare nanoparticle surfaces are first modified with an initiator, and then the polymerization proceeds via surface-initiated polymerization.[12–15] Atom transfer radical polymerization (ATRP) is a common, widely used radical polymerization synthesis approach.[12,13,15] Werne et al. reported the synthesis of PGNs using surface-initiated ATRP in bulk.[12] Similarly, Pyun et al. synthesized the PGNs using silica nanoparticles and polymerized multiple homopolymers and copolymers, including poly(styrene), poly(methacrylate), poly(styrene)-block-poly(*n*-butyl methacrylate), etc., using ATRP.[15] However, most of these approaches involve organic solvents and a relatively high concentration of metal catalysts.

Activators regenerated by electron transfer (ARGET) ATRP, are gaining increasing attention due to their eco-friendliness by using less metal catalyst and performing the reaction in a water-based solution.[16–18] We recently reported the synthesis of PGNs with poly(methyl methacrylate) corona and silica core using ARGET-ATRP in a water-based miniemulsion process, in which the grafting density and chain length could be controlled.[19]

Polymer chain entanglement is normally the primary mechanism for interactions between PGNs, controlled by graft density, i.e., the length and number of the grafted polymer chains.[24,25]

C. Yuan, F. Käfer, C. K. Ober
Department of Materials Science and Engineering
Cornell University
Ithaca, NY 14853, USA
E-mail: c.ober@cornell.edu

The ORCID identification number(s) for the author(s) of this article can be found under https://doi.org/10.1002/marc.202100629

DOI: 10.1002/marc.202100629

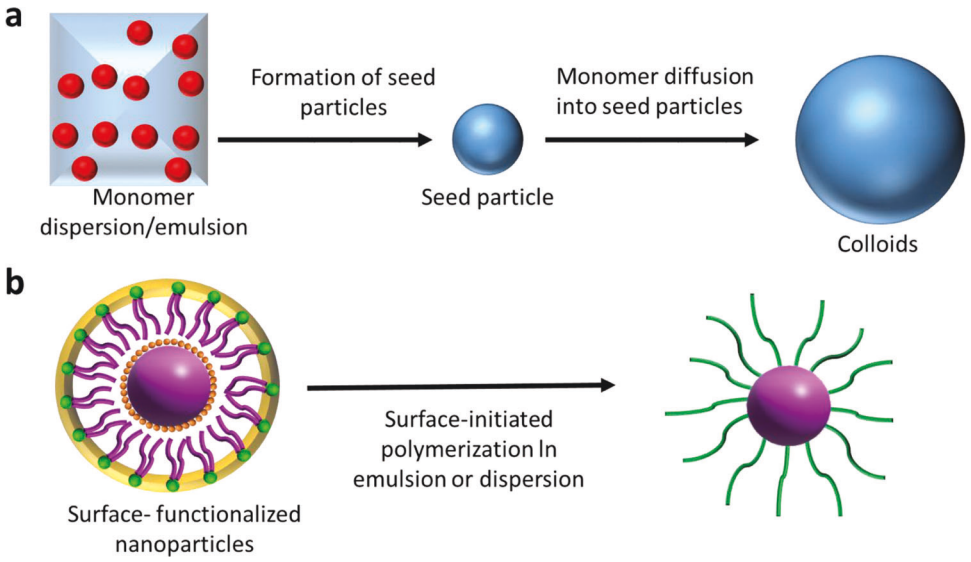

Scheme 1. a) Synthesis of polymeric colloids in dispersion b) surface-imitated polymerization of polymer nanoparticles and organic/inorganic nanoparticles.

However, for PGNs with very small diameters, grafted polymer chains are so short that entanglement is not normally sufficient to support the self-assembly and interaction of PGNs into robust 2D superlattice structures. The assembly of nanoparticle arrays and highly ordered superlattice structures of PGNs can instead be supported by more polar brushes through the formation of a variety of interparticle interactions, e.g., hydrogen bonding or ionic interactions instead of entanglements.[20–23] In such cases, additional interparticle interactions in addition to entanglement of polymer chains are complementary. Hydrogen bonds and ionic bonds among polymer chains could potentially be used to tailor the interparticle interactions and support the formation of PGNs monolayers. [21–23]

Here, we report the synthesis of PGNs with different polymer coronas containing hydrogen bonding sites. Both SiO_2-PDMAEMA and SiO_2-P4VP PGNs were chosen as the acceptors, while SiO_2-PVP PGNs derived from SiO_2-PAcS after hydrazinolysis were chosen as the donor. The synthesized PGNs were characterized using thermogravimetric analysis (TGA), and gel permeation chromatography (GPC) to determine the graft density. High-angle annular dark-field scanning transmission electron microscopy (HAADF-STEM) was used to characterize the core-shell structure, and bright-field transmission electron microscopy (BF-TEM) was used to characterize the structure of the particle assemblies.

2. Results and Discussion

Compared to the synthesis of polymeric colloids with a diameter of up to a few hundred nm, the synthesis of organic/inorganic hybrid nanoparticles such as polymer-grafted nanoparticles remains a challenge in terms of controllability of nanoparticle composition, morphology, and scalability of the synthesis. Moreover, the formation of ordered 2D and 3D superlattice structures is affected by the surface chemistry as well as the mechanical properties of the interactinvg PGN colloids. **Scheme 1** illustrates the differences in the synthesis strategies for the preparation of monodisperse colloids and organic/inorganic composite nanoparticles. Where monodisperse polymer particles can be synthesized using dispersion or emulsion polymerization, forming seed particles at the beginning of the polymerization which is swollen by monomer over time (Scheme 1a), organic/inorganic nanoparticles are typically synthesized using surface-initiated polymerization in dispersion, emulsion, or mini-emulsion where the polymerization is localized on the surface of the previously-modified nanoparticles (Scheme 1b).

In this work, polymer-grafted silica nanoparticles were synthesized using an aqueous-based ARGET ATRP reaction using a mini-emulsion approach, shown in **Scheme 2**. In the first step, silica nanoparticles were functionalized with the silane-based ATRP initiator APTES-BIBB. Second, the functionalized silica particles were emulsified in water and monomer as well as the reducing agent ascorbic acid was fed over time. To further control the place of polymerization and to enhance the monomer transport into the micelles, a quaternary ammonium salt, tetrabutylammonium bromide (TBAB), was used.[18,19] Using this synthesis approach the polymerization was localized onto the nanoparticle surface and the formation of ungrafted chains was suppressed. The synthesized PGNs were characterized by Fourier-transform infrared spectroscopy (FT-IR), suggesting the successful polymerization of the monomers on the particle surface, see Figure S1 in the Supporting Information. For the SiO_2-PDMAEMA PGNs, characteristic bands at (m, 1731 cm^{-1} –C=O); (m, 2775–2950 cm^{-1}, -$N(CH_3)_2$)) were observed. For SiO_2-P4VP PGNs characteristic bands of the pyridine ring can be found at (w, 1598, 1556, 1461, and 1416 cm^{-1}) are found. SiO_2-PAcS-grafted PGNs, are showing a characteristic carbonyl band at (m, –C=O, 1760 cm^{-1}) and a Ph-O stretching at (m, 1210 cm^{-1}).

To obtain the molar mass of the grafted polymers, the silica cores of the PGNs were removed by etching and GPC was used to determine the molar mass of the polymer chains. The polymer weight fraction was determined by TGA. Knowing the

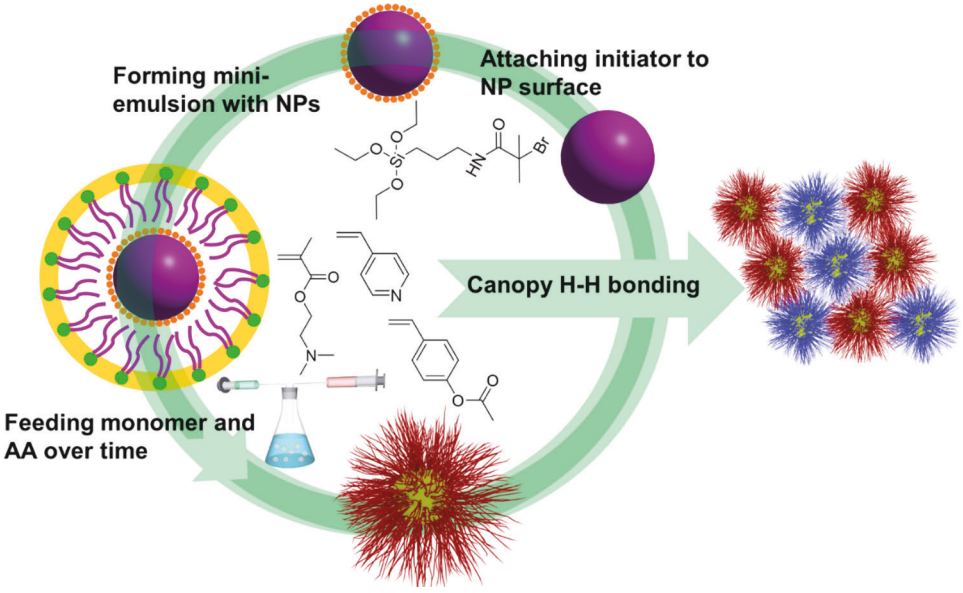

Scheme 2. Synthesis of PGNs with different polymer corona via mini-emulsion polymerization.

Table 1. PGNs synthesized with different polymer corona via surface initiated ARGET-ATRP mini-emulsion polymerization.

Sample	Molar mass [g mol^{-1}][a)]	Organic content [wt%]	Graft density [chains nm^{-2}][b)]	Monomer feeding rate [mmol h^{-1}][d)]	Diameter [nm][e)]
SiO_2-P4VP					
1	10 500	9.4	0.0113	2.35	71 ± 9
2	16 600	19.2	0.0416	9.4	78 ± 12
3	10 900	15.7	0.0431	4.7	119 ± 17
SiO_2-PDMAEMA					
4	14 800	11.7	0.0164	3.0	33 ± 3
5	13 200	14.3	0.0295	1.5	34 ± 2
6	12 900	17.1	0.0433	6.0	38 ± 16
SiO_2-PAcS					
7	130 100	22.6	0.0071	3.2	71 ± 12
8	129 400	25.3	0.0087	1.6	71 ± 9
9	132 100	37.6	0.0171	6.4	78 ± 10

[a)] molar mass of the former grafted chains after etching of the silica using HF [b)] calculated using Equation S1 in the Supporting Information [c)] initiator content was determined from TGA of functionalized particles with 7.1 wt% [d)] reaction time 8 h [e)] determined by DLS measurements in DMF at 25 °C.

weight fraction of grafted polymers and molecular weight determined by TGA (Supporting Information, Figure S2) and GPC (Supporting Information, Figure S3), respectively, the graft density (**Table 1**) was calculated using Equation S1 in the Supporting Information.[8]

Changing the total amount of monomer added over time allows the control of the polymer content, i.e., the resulting graft density. The graft density of all samples was varied in the range of 10^{-2}–10^{-3} chain nm^{-2}. For the SiO_2-P4VP (Sample 1–3) and grafted nanoparticles, the grafting density could be varied in the range from 0.0113 (Sample 1) up to 0.0431 chain nm^{-2} with a polymer content increasing from 9.4 wt% to 19.2 wt% with a nearly constant molar mass of the grafted chains between 10 kg mol^{-1} for Sample 1 and 16 kg mol^{-1} for Sample 3. A similar trend could be found for the synthesized SiO_2-PDMAEMA PGNs. Sample 4 has a graft density of 0.0164 chain nm^{-2} with a polymer content of 11.7 wt% and molar mass of approximately 15 kg mol^{-1} whereas the increase of the total amount of added monomer is resulting in a graft density for Sample 6 of 0.0433 chain nm^{-2} with a polymer content of 17.1 wt% and a molar mass of 13 kg mol^{-1} was obtained. It is worth noting, for the synthesis of SiO_2-P4VP PGNs the concentration of monomer was found to be significantly higher in comparison to SiO_2-DMAEMA to obtain PGNs with similar graft-densities, which is due to the difference in hydrophilicity. Interestingly, the synthesized SiO_2-PAcS PGNs have a lower graft density ranging from 0.0071 chain nm^{-2} (Sample 7) up to 0.0171 chains nm^{-2} with a significantly higher polymer content of up to 37.6 wt%

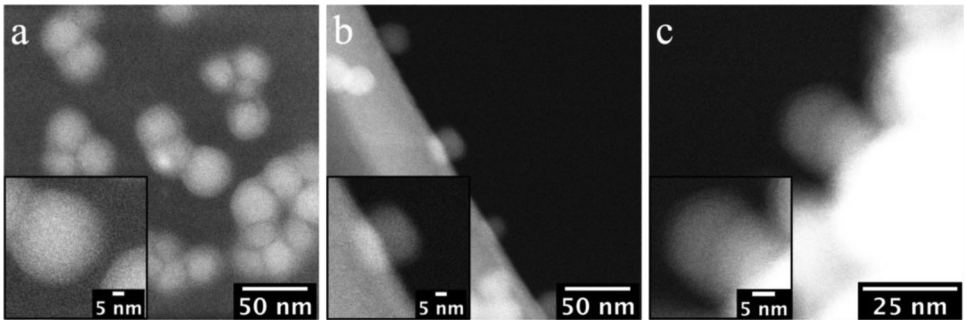

Figure 1. HAADF-STEM images of a) SiO2-P4VP (Sample 3) corona thickness 5.9 nm, b) SiO2-PDMAEMA (Sample 6) corona thickness 3.7 nm, c) SiO2-PAcS (Sample 9) corona thickness 2.6 nm.

and a molar mass of around 130 kg mol^{-1} (Sample 9) employing the same conditions used for the preparation of SiO_2-DMAEMA PGNs attributed to higher hydrophobicity of acetoxy styrene.

HAADF-STEM was used to show the polymer corona grafted on the particle surface. **Figure 1** shows the STEM images of samples 3, 6, and 9. The corona thickness was calculated by subtracting the core radius from the outer radius of individual PGNs as viewed in STEM. The corona thickness of SiO_2-P4VP PGNs with the highest graft density of 0.0431 chains nm^{-2} (Sample 3, Table 1) was 5.9 nm. In contrast, for SiO_2-PDMAEMA PGNs (Sample 6, 0.0433 chain nm^{-2}) with a similar graft density compared to (Sample 1, 0.0431 chains nm^{-2}) the corona thickness is around 3.7 nm. The corona thickness of SiO_2-PAcS PGNs (Sample 9, 0.0171 chains nm^{-2}) was determined as 2.6nm. However, SiO_2-PAcS PGNs tended to aggregate due to the high polymer content and molar mass of the grafted chains. This has been previously observed for SiO_2-PMMA PGNs, with a polymer content above 30 wt%.[19]

Whereas the self-assembly of polymeric colloid micro-and nanoparticles is well studied,[26] the formation of 2D and 3D superlattice structures of PGNs is affected by factors such as the nanoparticle size, graft density, the molar mass of the grafted chains as well as the properties and interparticle interactions of the polymer chains.[27]

Dynamic light scattering (DLS) measurements of the synthesized PGNs are showing a narrow size distribution and an increasing diameter with increasing graft density confirming the successful polymerization of a polymer corona on silica particles, see Supporting Information, Figure S4. For the SiO_2-PDMAEMA PGNs samples, the diameter is increasing from 33 nm (Sample 7, graft density 0.0164 chains nm^{-2}) up to around 39 nm (Sample 9, graft density 0.0433 chains nm^{-2}). It is worth noting, that the diameters for SiO_2-P4VP and SiO_2-PAcS are significantly higher than determined from TEM due to the swelling of the polymer corona.

For the formation of ordered assembly structures using PGNs with a low graft density in the range 10^{-2}–10^{-3} chains nm^{-2}, interparticle interactions can play an essential role. The hydrogen-bonding interaction between SiO_2-P4VP and SiO_2-PVP, as well as between SiO_2-PDMAEMA and SiO_2-PVP were evaluated as potential hydrogen bonding acceptor/donor systems. Therefore, the resulting SiO_2-PAcS-grafted PGNs (Sample 8) was deprotected using hydrazine to form hydroxy groups (-OH), which can serve as hydrogen bonding sites. The obtained SiO_2-PVP PGNs were characterized by FT-IR measurements, see Supporting Information, Figure S5. The appearance of the band at 2800–3600 cm^{-1} corresponding to the hydroxy groups (w, -OH) of the deprotected SiO_2-PAcS, and the disappearance of the carbonyl band (m, 1700 cm^{-1}, –C═O) confirmed the successful deprotection. The post-polymerization deprotection reaction and the resulting hydroxyl groups enable the formation of interparticle hydrogen bonding interactions between the -OH group of the SiO_2-PVP PGNs and SiO_2-P4VP/PDMAEMA PGNs.

PGN assemblies of SiO_2-P4VP PGNs (Sample 1, graft density = 0.0113 chains nm^{-2}; and Sample 2, graft density = 0.0416 chains nm^{-2}), and SiO_2-PDMAEMA PGNs (Sample 4, graft density = 0.0164 chains nm^{-2}), respectively, were prepared on carbon film on TEM grids. The assemblies of these particles mixed with SiO_2-PVP PGNs (Sample 8, graft density = 0.0087 chains nm^{-2}) at a mass ratio of 1:1, respectively, were also prepared using the same method and condition. The particles were dispersed in anhydrous toluene by ultrasonication, and the particle assemblies were prepared simply by drop-casting. **Figure 2** shows the TEM images of the obtained PGN assemblies on carbon film on TEM grids.

When compared with their binary counterparts which involve the hydrogen bonding donor SiO_2-PVP PGNs (Figure 2a,c,e), the PGN assemblies with single-particle components (Figure 2b,d,f) have higher irregularity as the particles are randomly ordered and overlap with each other. On the contrary, the binary donor/acceptor particle assemblies are more likely to form interparticle hydrogen bondings which result in more dense packing as well as more ordered structures. Moreover, it was observed that upon the addition of the donor SiO_2-PVP particles, the regularity of binary assembly of acceptor SiO_2-P4VP PGNs with lower grafting density (Figure 2a) was reduced compared to assemblies using PGNs with a higher grafting density (Figure 2c). Therefore, varying the graft density of the PGNs seems to change the number of the interparticle hydrogen bondings, and thus, the regularity of the PGN assembly. This effect, however, must be further studied by preparing particle assemblies consisting of PGNs with different combinations of chain lengths, diameters, and particle cores.

3. Conclusion

In this work, SiO_2-P4VP, SiO_2-PDMAEMA, and SiO_2-PAcS PGNs were synthesized using silica cores of 25-nm diameter

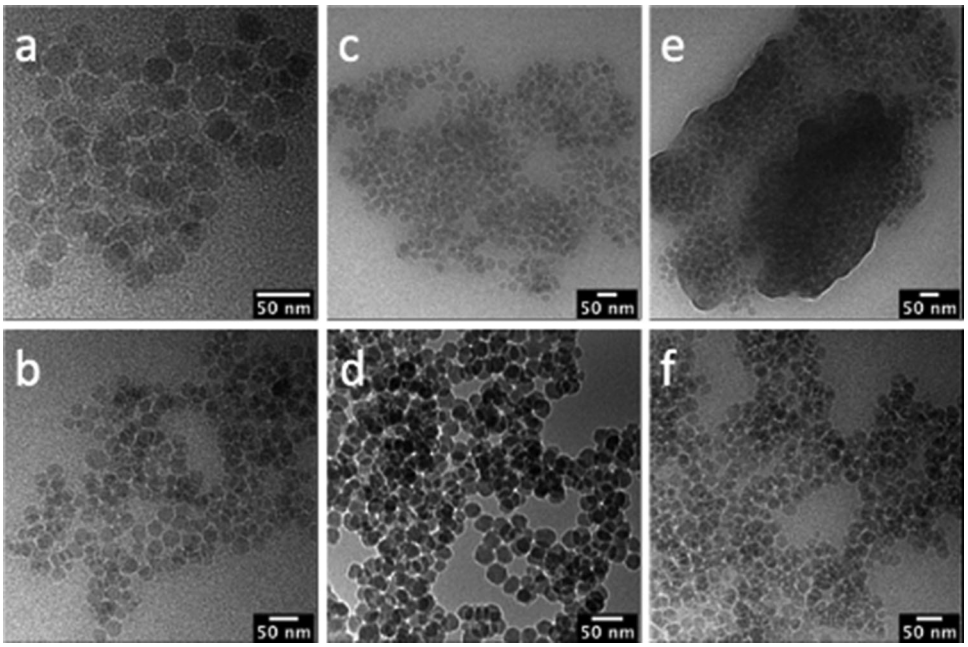

Figure 2. TEM image of a) SiO_2-PVP PGNs (Sample 8, graft density = 0.0087 chains nm^{-2}) mixed with SiO_2-P4VP PGNs (Sample 1, graft density = 0.0113 chains nm^{-2}); b) SiO_2-P4VP PGNs (Sample 1, graft density = 0.0113 chains nm^{-2}); c) SiO_2-PVP PGNs (Sample 8, graft density = 0.0087 chains nm^{-2}) mixed with SiO_2-P4VP PGNs (Sample 2, graft density = 0.0416 chains nm^{-2}); d) SiO_2-P4VP PGNs (Sample 2, graft density = 0.0416 chains nm^{-2}); e) SiO_2-PVP PGNs (Sample 8, graft density = 0.0087 chains nm^{-2}) mixed with SiO_2-PDMAEMA PGNs (Sample 4, graft density = 0.0164 chains nm^{-2}) f) SiO_2-PDMAEMA PGNs (Sample 4, graft density = 0.0164 chains nm^{-2}).

by using ARGET-ATRP in a mini-emulsion like a synthesis approach. The graft density of the synthesized PGNs varied between the magnitude of 10^{-2}–10^{-3} chain nm^{-2} depending on the total amount of monomer added. Furthermore, the PGNs were characterized using HAADF-STEM showing a clear polymer-corona with a diameter of 5.9 nm for SiO_2-P4VP (Sample 1), 3.7 nm for SiO_2-PDMAEMA (Sample 3), and 2.6 nm for SiO_2-PAcS (Sample 9). Dynamic light scattering measurements show a narrow particle size distribution, while hydrodynamic diameter increases with increasing graft density confirming the successful polymerization of polymer coronas. To support the formation of ordered PGN structures, interparticle hydrogen bonding between SiO_2-PDMAEMA and SiO_2-PVP, as well as between SiO_2-P4VP and SiO_2-PVP were utilized. Therefore, the SiO_2-PAcS PGNS was deprotected via hydrazinolysis resulting in SiO_2-PVP PGNs, with hydroxy groups acting as hydrogen bond donors. PGN assemblies were prepared directly on carbon film on TEM grids. While SiO_2-PDMAEMA and SiO_2-P4VP PGNs themselves formed assemblies with high irregularity, mixing these hydrogen bonding acceptor particles with SiO_2-PVP particles led to the formation of more ordered structures. However, further studies are required to investigate the effect of hydrogen interparticle hydrogen bonds on the formation and structure of 2D and 3D superlattice PGNs structures.

4. Experimental Section

Materials: (3-Aminopropyl) triethoxysilane (APTES) (99%), triethylamine (99%), 2-bromo-2-methylpropionyl bromide (BIBB) (98%), magnesium sulfate (anhydrous), Dowex 50W X8 ion-exchange resin (50-100 mesh), Dowex 1X 8 ion-exchange resin (50-100 mesh), sodium hydroxide (reagent grade), HCl aqueous solution (37%), Ludox TM-40 particles dispersion (40%), dioxane (99%) and hydrazine monohydrate (98%) were purchased from Sigma-Aldrich and used as received. Tetrahydrofuran (THF) (ACS grade), dichloromethane (DCM) (ACS grade), methanol (ACS grade), anhydrous toluene and dimethylformamide (DMF) (ACS grade) were purchased from Fisher Scientific and used as received. Pluronic F-127, TBAB (98%), Copper (II) bromide (99%, extra pure, anhydrous), and L-ascorbic were purchased from Acros Organics and used as received. Inhibitor removal resin was purchased from Alfa Aesar and used as received. 4-Acetoxystyrene (96%, stabilized), 4-vinyl pyridine (95%, stabilized), 2-dimethylamino ethyl methacrylate (99% stabilized) were also purchased from Acros Organics and destabilized by passing through the inhibitor remover three times shortly before use. Tris(2-pyridylmethyl) amine (TPMA, 98%) was purchased from TCI. The water used in all experiments was generated by a Millipore Sigma Milli-Q IQ 7000 Ultrapure Water System, with a resistivity of 18.2 MΩ•cm.

Synthesis and Characterization of the Initiator APTES-BIBB: The initiator APTES-BIBB was synthesized for functionalizing the surface of silica nanoparticles. APTES (2.2137 g, 10 mmol), triethylamine (3.86 mL, 28 mmol), and THF (170 mL) were added into a 500mL round bottom flask. The flask was dipped into an ice bath to be cooled to 0 °C. BIBB (3.18 g, 0.014 mol) was dissolved in 30mL THF and dropped into the flask with a dropping funnel under stirring for 30 minutes. Then the ice bath was removed, and the solution was kept stirring overnight. After that, the solution was turbid with a white precipitate formed. The solution was filtered to remove the white precipitate, and the rotary evaporated to remove the excess solvent. A yellow oily liquid remained and was dissolved in DCM (40 mL). The mixture was then washed with saturated sodium bicarbonate solution and cold water, alternatively, four times using a separatory funnel. The organic phase was collected, and an excess amount of anhydrous magnesium sulfate was added to remove the residue water. The excess DCM was removed by a rotary evaporator, and APTES-BIBB was obtained and stored at -20 °C until further use.

Preconditioning of Ludox TM-40 Particles: The steps in this section were to precondition the commercial silica nanoparticles to make their surfaces suitable for grafting initiators. Dowex 50W X8 ion-exchange resin and Dowex 1X8 ion-exchange resin (both 50 g) were transferred to two separate 600 mL beakers. The resins were washed with NaOH (3 N), hot water, methanol, and cold water, in sequence for five cycles. Between every two washes, the resins were collected by filtration. After the last wash cycle of Dowex 50W X8, the resin was washed with an excess amount of HCl (3 N) solution to convert the resin to the hydrogen form. Similarly, Dowex 1X8 was washed with an excess amount of NaOH (3 N) solution to convert to the hydroxy form. Then both were washed with water. Shortly after the conversion, the Dowex 50W X8 was mixed with Ludox TM-40 dispersion (100 mL) and water (100 mL). The mixture was kept stirring overnight. The Ludox TM-40 dispersion was then collected via filtration, added to Dowex 1X8 resin, and stirred overnight again. The particle dispersion was then collected via filtration and centrifuged at 3000 rpm to remove the large aggregates. The dispersion was then dialyzed against ethanol for 1 week with the ethanol being changed every 24 hours.

Functionalization of Ludox TM-40 with APTES-BIBB: The steps in this section were to functionalize the surface of the silica nanoparticles with the synthesized initiators. Preconditioned Ludox TM-40 particles (10 g) were mixed with toluene (500 mL) in a round bottom flask. The mixture was sonicated until the particles were well dispersed in toluene. APTES-BIBB (8 g) was added into the flask and the mixture was kept stirring at 50 °C for 24 hours. After 24 hours, the particles were collected by centrifuging at 4400 rpm, washed with toluene (50 mL) 4 times, and DCM (50 mL) 4 times. Between every two washes, the particles were collected by centrifuging at 4400 rpm and the supernatant was disposed of. Finally, the particles were dried in a vacuum oven overnight.

Synthesis of Polymer-Grafted Nanoparticles (PGNs): The synthesis method of polymer-grafted nanoparticles was described using Sample 1, Table 1 as an example. Functionalized SiO_2-APTES-BIBB particles (200 mg) were mixed with Pluronic F-127 aqueous solution (0.08 g mL^{-1}, 10 mL) in a 20 mL scintillation vial. The vial was then vortexed by a vortex mixer and sonicated by an ultrasonic bath for 30 minutes until a milky white dispersion formed. Parallelly, TBAB (1.934 g, 6 mmol), TPMA (20.8 mg, 71.6 µmol), $CuBr_2$ aqueous solution (1 mg mL^{-1}, 2 mL) and water (43.2 mL) were added into a 100 mL round bottom flask. The particle dispersion was then added into the flask and a stirring bar was also added. The flask was sealed using a rubber septum and purged with argon for 30 minutes for degassing. 4-vinyl pyridine (2 mL, 18.8 mmol, 2.35 mmol h^{-1}) and L-ascorbic acid aqueous solution (18 mM, 4.8 mL, 10.8 µmol h^{-1}) were then prepared and fed into the flask at constant rates over 8 hours period at 80 °C using two separate syringe pumps. After 8 hours, the polymerization was terminated by opening the flask to air. The particles were then collected by centrifuging at 4400 rpm and washed with water (50 mL, 3 times) and THF (50 mL, three times). Between every two washes, the particles were collected by centrifuging at 4400 rpm and the supernatant was disposed. Finally, the particles were dried in a vacuum oven overnight at 70 °C.

Hydrazinolysis of Poly (4-Acetoxystryene)-Grafted Nanoparticles: SiO_2-PAcS particles (Sample 8) (50 mg) were mixed with dioxane (10 mL) in a 20 mL scintillation vial and sonicated until the particles dispersed well. Hydrazine monohydrate (100 µL, 20.61 µmol) was dropped into the vial slowly. The mixture was kept stirring for 24 hours. After 24 hours, the particles were collected by centrifuging at 10 000 rpm and washed with dioxane (15 mL) 3 times. Between every two washes, the particles were collected by centrifuging at 10 000 rpm and the supernatant was disposed of. Finally, the particles were dried in a vacuum oven overnight at 70 °C.

Preparation of PGN Assemblies: The PGNs were dispersed in anhydrous toluene with 1 mg mL^{-1} particle concentration by ultrasonication, and the self-assembly was conducted on carbon film on TEM grid by drop-casting.

Characterizations: TGA was performed on a TA Instruments Inc. Q500. The samples were heated from room temperature to 800 °C with a heating rate of 10 °C min^{-1} under a nitrogen atmosphere.

The molar mass and dispersity of the grafted polymer chains were measured after HF etching by GPC using THF as eluent. One precolumn (SDV; particle size 3 µm, dimension 8.0 mm·50 mm), two PSS SDV columns (particle size 3 µm, dimension 8.0 mm·300 mm, 1000 Å) and one PSS SDV column (particle size 3 µm, dimension 8.0 mm·300 mm, 10000 Å) were used. Polystyrene of different molar masses with narrow dispersity was used as standards. The flow rate was set at 1.0 mL min^{-1}. A differential refractive index detector was used as the detector. The software PSS WinGPC 6 was used to determine the molar mass and disparity of the measured samples.

DLS was performed on a Malvern Panalytical Inc. ZetaSizer 90. The dynamic light scattering was measured for particles dispersed in DMF at 25 °C.

FT-IR measurements were performed on a Bruker Vertex V80V Vacuum FTIR system. PGNs aggregated were firstly grounded into fine powders and the powders were measured by FTIR at 2 cm^{-1} resolutions in the range between 4000 and 400 cm^{-1}, with an integrating time of 1 minute for each sample. Depending on the polymer composition, PGNs showed different characteristic peaks.

BF-TEM and HAADF-STEM images were captured by FEI F20 TEM STEM with a Thermo-Fisher GF20 scope, monochromated and operated at 200 kV.

Supporting Information

Supporting Information is available from the Wiley Online Library or from the author.

Acknowledgements

C.Y. and F.K. contributed equally to this work. The authors would like to extend their gratitude to the Air Force Office of Scientific Research (AFOSR FA9550-17-1-0038), and the Air Force Research Laboratory for prior support. This work made use of the Cornell Center for Materials Research Shared Facilities, which is supported through the NSF MRSEC program (DMR-1719875) and Cornell Energy Systems Institute (CESI).

Conflict of Interest

The authors declare no conflict of interest.

Data Availability Statement

The data that supports the findings of this study are available in the supplementary material of this article

Keywords

ARGET-ATRP, core-shell particles, emulsion polymerization, hydrogen bonding, polymer-grafted nanoparticles

Received: September 19, 2021
Revised: November 2, 2021
Published online:

[1] M. V. Kovalenko, L. Manna, A. Cabot, Z. Hens, D. V. Talapin, C. R. Kagan, V. I. Klimov, A. L. Rogach, P. Reiss, D. J. Milliron, P. Guyot-Sionnnest, G. Konstantatos, W. J. Parak, T. Hyeon, B. A. Korgel, C. B. Murray, W. Heiss, *ACS Nano* **2015**, *9*, 1012.
[2] B. Lebeau, P. Innocenzi, *Chem. Soc. Rev.* **2011**, *40*, 886.

[3] H. Sabouri, K. Ohno, S. Perrier, *Polym. Chem.* **2015**, *6*, 7297.
[4] X. Ye, L. Qi, *Sci. China: Chem.* **2013**, *57*, 58.
[5] M. Egen, R. Zentel, *Macromol. Chem. Phys.* **2004**, *205*, 1479.
[6] F. Fleischhaker, R. Zentel, *Chem. Mater.* **2005**, *17*, 1346.
[7] F. Fleischhaker, A. C. Arsenault, V. Kitaev, F. C. Peiris, G. von Freymann, I. Manners, R. Zentel, G. A. Ozin, *J. Am. Chem. Soc.* **2005**, *127*, 9318.
[8] C. I. C. Crucho, M. T. Barros, *Mater. Sci. Eng., C* **2017**, *80*, 771.
[9] S. K. Kumar, B. C. Benicewicz, R. A. Vaia, K. I. Winey, *Macromolecules* **2017**, *50*, 714.
[10] M. J. A. Hore, L. T. J. Korley, S. K. Kumar, *J. Appl. Phys.* **2020**, 128, 030401.
[11] M. J. A. Hore, *Soft Matter* **2019**, *15*, 1120.
[12] T. von Werne, T. E. Patten, *J. Am. Chem. Soc.* **1999**, *121*, 7409.
[13] K. Ohno, T. Morinaga, K. Koh, Y. Tsujii, T. Fukuda, *Macromolecules* **2005**, *38*, 2137.
[14] C. Li, J. Han, C. Y. Ryu, B. C. Benicewicz, *Macromolecules* **2006**, *39*, 3175.
[15] J. Pyun, S. Jia, T. Kowalewski, G. D. Patterson, K. Matyjaszewski, *Macromolecules* **2003**, *36*, 5094.
[16] W. Jakubowski, K. Min, K. Matyjaszewski, *Macromolecules* **2006**, *39*, 39.
[17] A. Simakova, S. E. Averick, D. Konkolewicz, K. Matyjaszewski, *Macromolecules* **2012**, *45*, 6371.
[18] R. Cordero, A. Jawaid, M.-S. Hsiao, Z. Lequeux, R. A. Vaia, C. K. Ober, *ACS Macro Lett.* **2018**, *7*, 459.
[19] D. Y. Wu, F. Käfer, N. Diaco, C. K. Ober, *J. Polym. Sci.* **2020**, *58*, 2310.
[20] C. Yi, Y. Yang, B. Liu, J. He, Z. Nie, *Chem. Soc. Rev.* **2020**, *49*, 465.
[21] H. Yao, H. Kojima, S. Sato, K. Kimura, *Langmuir* **2004**, *20*, 10317.
[22] D. Luo, C. Yan, T. Wang, *Small* **2015**, *11*, 5984.
[23] P. J. Santos, R. J. Macfarlane, *J. Am. Chem. Soc.* **2020**, *142*, 1170.
[24] N. J. Fernandes, H. Koerner, E. P. Giannelis, R. A. Vaia, *MRS Commun.* **2013**, *3*, 13.
[25] Y. Jiao, A. Tibbits, A. Gillman, M.-S. Hsiao, P. Buskohl, L. F. Drummy, R. A. Vaia, *Macromolecules* **2018**, *51*, 7257.
[26] P. Ferrand, M. Egen, B. Griesebock, J. Ahopelto, M. Müller, R. Zentel, S. G. Romanov, C. M. S. Torres, *Appl. Phys. Lett.* **2002**, *81*, 2689.
[27] N. K. Hansoge, A. Gupta, H. White, A. Giuntoli, S. Keten, *Macromolecules* **2021**, *54*, 3052.